Iranian Journal of Chemical Engineering
Vol. 3, No. 4 (Autumn), 2006, IAChE

Determination of the Kinetic Parameters and Dynamic Modeling of the Reactor for the Direct Conversion of Synthesis gas to Di-methyl ether

*A. Hadipour, M. Sohrabi**
Department of Chemical Engineering, Amirkabir University of Technology, Tehran 159145, Iran.

Abstract

In the present study the reaction kinetic and dynamic modeling of the reactor for syngas transformation into dimethyl ether using a mixture of a metallic oxides (CuO, ZnO, Al_2O_3), and an acidic component (γ-Al_2O_3) as the catalyst has been investigated. A combination of the Graff kinetic model for methanol synthesis and the Bercic model for methanol dehydration was correlated with the experimental results obtained in this study. Activity and kinetic measurements were carried out using a catalytic fixed bed micro reactor. The operating temperature range was 230-300 ℃ and the pressure was 8 barg. The experimental runs were performed applying a wide range of catalyst to feed ratios. A simple dynamic model for the reactor performance was developed and tested with the experimental data. The mean absolute deviation, concerning the data for the steady state conditions, was less than 8%.

Keywords: *DME , kinetic parameter, fixed bed reactor, dynamic modeling*

1. Introduction

Dimethyl ether (DME) is an intermediate in the preparation of a number of industrial chemicals. It has also found increasing application in the aerosol industry as an ozone friendly propellant. In addition, DME is used as an ultra-clean fuel for diesel engines [1-3].
Commercial production of dimethyl ether is achieved using either of the following two methods, 1) a two-step procedure consisting of methanol formation from synthesis gas followed by the dehydration of the latter, and 2) a single step process that is the direct formation of DME from synthesis gas. In comparison with the two-step method, the single-step procedure is attracting more attention for its dramatic economic value and theoretical significance [4].
A bifunctional catalyst for the conversion of synthesis gas to DME normally contains two types of active sites used for methanol formation and methanol dehydration, respectively. These catalysts usually contain zinc, copper and aluminum oxides (for methanol formation) and gamma-alumina as a zeolite (for methanol dehydration), and are prepared by the co-precipitation method [5].
DME can be obtained directly from synthesis gas according to the following reactions:

* - Corresponding author: E-mail: sohrabi@aut.ac.ir

$$\text{I)}\quad CO + 2H_2 \Leftrightarrow CH_3OH \qquad \text{(Methanol Synthesis)}$$
$$\text{II)}\quad CO_2 + 3H_2 \Leftrightarrow CH_3OH + H_2O \qquad \text{(Methanol Synthesis)}$$
$$\text{III)}\quad CO + H_2O \Leftrightarrow CO_2 + H2 \qquad \text{(Water Gas Shift Reaction)}$$
$$\text{IV)}\quad 2CH_3OH \Leftrightarrow CH_3OCH_3 + H_2O \qquad \text{(Dehydration of Methanol to DME)}$$
$$\text{V)}\quad 2CO + 4H_2 \Leftrightarrow CH_3OCH_3 + H_2O \qquad \text{(Direct Synthesis of DME)}$$

In the present study, the reaction kinetic parameters have been determined and the dynamic modeling of reactor performance for DME synthesis from syngas has been developed and correlated with the experimental results.

2. Experimental

The activity of catalysts in converting synthesis gas to DME were studied under both unsteady and steady state conditions in a fixed bed flow reactor (i.d., 6.4mm and length 650 mm) connected online to a GC apparatus. The catalyst was prepared according to the procedure given in reference 6 and packed in a stainless steel tubular reactor equipped with a thermocouple placed in the catalyst bed. Experiments were performed in temperatures ranging from 230-300ºC and a constant pressure of 8 barg. Prior to catalytic testing, the samples were crushed and sieved to fine powders. In each experimental run, about 2 grams of catalyst (grain size equal to 150 μm) was loaded in the reactor having two stainless steel supports at both ends of the catalyst bed. A schematic diagram of the experimental rig is shown in Figure 1. The reactor system was first purged with nitrogen gas and then pressurized. The catalysts were reduced in a flowing hydrogen gas diluted with nitrogen.

A mixture of 4 vol. % CO_2, 32 vol. % CO and 64 vol. % H_2 entered the top section of the reactor that acted as a pre-heater. Three mass flow meters (Brooks, Model 5850) and a control system were used to monitor the individual gas flow rates and to provide the required gas mixtures.

A portion of the effluent gas, after reducing its pressure by a back pressure regulator, was directed to a gas chromatograph apparatus (Agilent- 6890) connected online to the system. The effluent gas was analyzed several times with four to seven minute intervals during each experimental run. The GC column was packed with Porapak Q with 80–100 mesh. The column temperature was increased steadily from 70 to 200°C and remained at that level for 4 minutes. Helium was used as a carrier gas with a flow rate of 2.5 cm^3/min. The thermal conductivity detector was applied.

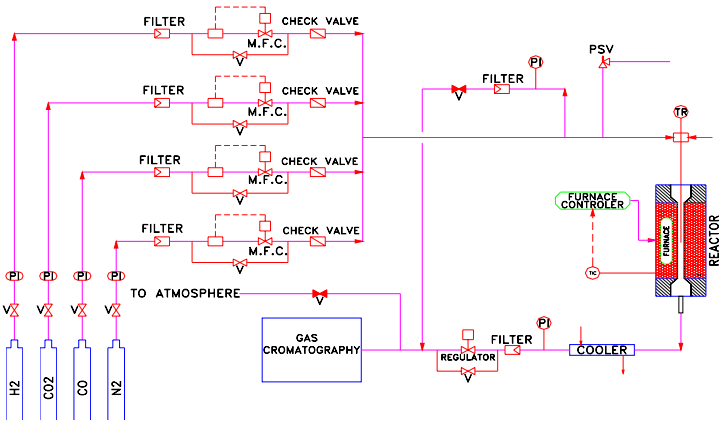

Figure 1. The schematic diagram of the reactor setup.

3. Results and discussion

The reaction has been carried out within a temperature range of 230-300 °C, 8 barg pressure and a wide range of catalyst to feed ratios. The results are presented in Fig.2 and Tables 1-4.

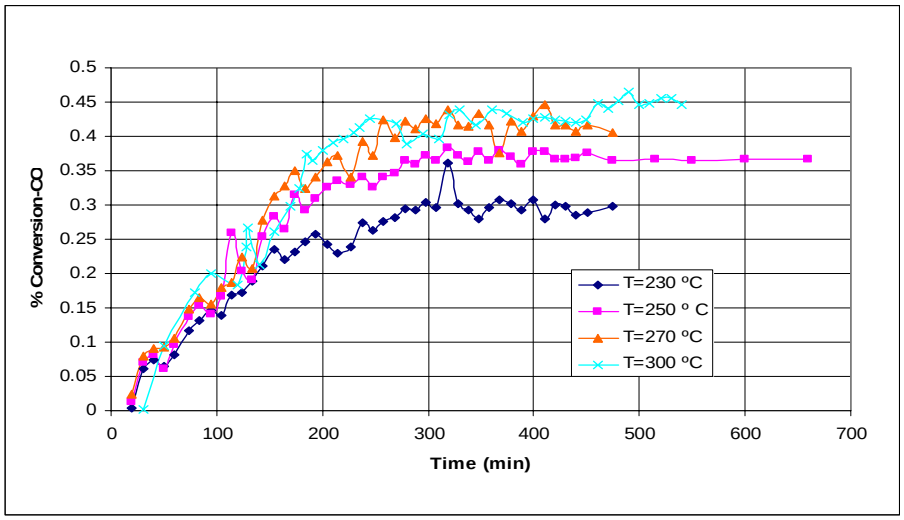

Figure 2. Conversion of Co as a function of time (at different temperatures).

Table 1. Data for the reactor's outlet stream at 230 °C.

$W_{cat.}/F_{CO}$	$W_{cat.}/\phi_v$	P_{H_2}	P_{CO}	P_{CO_2}	P_{CH_3OH}	P_{DME}	P_{H_2O}	$-r_{CO}$	r_{DME}
$^{gr}/_{(mol/\min)}$	$^{gr}/_{(m^3/\min)}$	barg	barg	barg	barg	barg	barg	$^{mol}/_{(\min .gr)}$	$^{mol}/_{(\min .gr)}$
260	3731	4.96	2.47	0.32	0.003	0.13	0.12	3.3E-04	1.5E-04
896	12658	4.60	2.29	0.48	0.03	0.30	0.30	1.2E-04	5.7E-05
1120	15873	4.55	2.26	0.46	0.04	0.35	0.34	1.0E-04	4.5E-05
1493	21052	4.43	2.20	0.52	0.07	0.40	0.36	7.4E-05	3.4E-05
1792	25316	4.39	2.17	0.51	0.09	0.43	0.41	6.3E-05	2.9E-05
2240	31746	4.34	2.15	0.49	0.13	0.45	0.44	5.3E-05	2.5E-05

Table 2. Data for the reactor's outlet stream at 250 °C.

No	$W_{cat.}/F_{CO}$	$W_{cat.}/\phi_v$	P_{H_2}	P_{CO}	P_{CO_2}	P_{CH_3OH}	P_{DME}	P_{H_2O}	$-r_{CO}$	r_{DME}
	$^{gr}/_{(mol/\min)}$	$^{gr}/_{(m^3/\min)}$	barg	barg	barg	barg	barg	barg	$^{mol}/_{\min .gr}$	$^{mol}/_{\min .gr}$
1	260	3731	4.91	2.45	0.33	0.004	0.16	0.15	3.2 E-4	2.2 E-4
2	896	12658	4.47	2.21	0.50	0.04	0.40	0.38	1.3E-4	8.8E-5
3	1120	15873	4.40	2.18	0.48	0.05	0.45	0.43	1.1 E-4	7.2E-5
4	1493	21052	4.24	2.1	0.56	0.08	0.52	0.5	8.7E-5	5.5E-5
5	1792	25316	4.18	2.06	0.55	0.11	0.56	0.54	7.6E-5	4.8E-5
6	2240	31746	4.11	2.02	0.53	0.16	0.60	0.58	6.5E-5	4.1E-5

Table 3. Data for the reactor's outlet stream at 270 °C.

$W_{cat.}/F_{CO}$	$W_{cat.}/\phi_v$	P_{H_2}	P_{CO}	P_{CO_2}	P_{CH_3OH}	P_{DME}	P_{H_2O}	$-r_{CO}$	r_{DME}
$^{gr}/_{(mol/\min)}$	$^{gr}/_{(m^3/\min)}$	barg	barg	barg	barg	barg	barg	$^{mol}/_{(\min.gr)}$	$^{mol}/_{(\min.gr)}$
260	3731	5.00	2.39	0.40	0.003	0.14	0.07	4.7E-04	2.1E-04
896	12658	4.71	2.07	0.67	0.03	0.36	0.17	1.8E-04	8.3E-05
1120	15873	4.69	2.00	0.69	0.04	0.40	0.17	1.4E-04	6.8E-05
1493	21052	4.58	1.89	0.79	0.07	0.46	0.20	1.1E-04	5.1E-05
1792	25316	4.55	1.85	0.80	0.10	0.50	0.21	9.2E-05	4.4E-05
2240	31746	4.52	1.78	0.82	0.14	0.53	0.21	7.5E-05	3.8E-05

Table 4. Data for the reactor's outlet stream at 300 °C.

$W_{cat.}/F_{CO}$	$W_{cat.}/\phi_v$	P_{H_2}	P_{CO}	P_{CO_2}	P_{CH_3OH}	P_{DME}	P_{H_2O}	$-r_{CO}$	r_{DME}
$^{gr}/_{(mol/\min)}$	$^{gr}/_{(m^3/\min)}$	barg	barg	barg	barg	barg	barg	$^{mol}/_{(\min.gr)}$	$^{mol}/_{(\min.gr)}$
260	3731	5.06	2.35	0.44	0.003	0.13	0.01	3.7E-04	1.7E-04
896	12658	4.86	1.97	0.78	0.03	0.33	0.30	1.3E-04	7.0E-05
1120	15873	4.87	1.89	0.82	0.04	0.37	0.01	1.0E-04	5.9E-05
1493	21052	4.80	1.76	0.94	0.07	0.43	0.003	7.6E-05	4.6E-05
1792	25316	4.78	1.71	0.96	0.09	0.46	0.003	6.6E-05	4.0E-05
2240	31746	4.74	1.63	0.98	0.13	0.50	0.01	5.4E-05	3.3E-05

The reaction rates given in these tables were calculated, assuming the plug flow of gas in the reactor, i. e.

$$-r_{CO} = \frac{d(X_{CO})}{d(W/F_{CO_0})} \tag{1}$$

$$r_{DME} = \frac{d\left(\frac{y_{DME.out}.P}{RT}\right)}{d\left(W/\phi_v\right)} \tag{2}$$

4. Developing the Model

4-1. Kinetic study

A number of studies on syngas transformation into liquid hydrocarbons have been reported [10-14]. A method similar to those proposed by Graaf and Bercic for complex reactions in isothermal fixed bed micro reactors was adopted in the present study. The Graff kinetic model has been used for the transformation of syngas to methanol, and that of Bercic has been applied in the synthesis of DME from methanol. These are as follows:

a- Graff model:

$$-r_{CO} = \frac{k_1\left[P_{CO}.P_{H_2}^{3/2} - P_{CH_3OH}/(P_{H_2}^{1/2}.k_{P1})\right]}{(1+k_2P_{CO}+k_3P_{CO_2})(P_{H_2}^{1/2}+k_4P_{H_2O})} \tag{3}$$

b- Bercic model:

$$r_{DME} = \frac{-k_5(P_{CH_3OH}^2 - P_{H_2O}.P_{DME}/K_{P2})}{(1+2(k_6P_{CH_3OH})^{1/2}+k_7P_{H_2O})^4} \tag{4}$$

Estimation of values for the kinetic para-

meters involved minimization of error. Using the nonlinear regression analysis and applying the results presented in Tables 1-4 to the relations 3 and 4, the kinetic parameters have been calculated. These are given in Table 5.

Table 5. Kinetic parameters.

Kinetic constant	*Temperature* $(^{\circ}C)$				K_{0I}	*E/R*
	230	*250*	*270*	*300*		
K_1	*8.68E-06*	*4.2E-05*	*2.6E-05*	*1.21E-05*	*1.1E-11*	*-7963.0*
K_2	*0.23479*	*0.32373*	*0.445121*	*0.54672*	*2.9E+02*	*3561.6*
K_3	*5.56758*	*3.32369*	*1.164179*	*0.947483*	*9.6E-07*	*-7812.4*
K_4	*4.95952*	*3.391903*	*0.258108*	*0.010129*	*8.2E-23*	*-26755.0*
K_{P1}	*0.027044*	*0.021084*	*0.011935*	*0.007082*	*2.5E-07*	*-5855.5*
K_5	*0.007663*	*0.005647*	*0.003643*	*0.001*	*6.1E-10*	*-8322.8*
K_6	*7.7855*	*11.05514*	*31.29*	*46.7116*	*5.4E+07*	*7940.1*
K_7	*8.38936*	*6.810235*	*6.19*	*5.13949*	*1.7E-01*	*-1957.2*
K_{P2}	*0.022624*	*0.017347*	*0.008427*	*0.00742*	*1.3E-06*	*-4880.6*

4-2. Reactor study

Assuming no axial dispersion, negligible inter particle and intera particle diffusional limitations, and also accounting for the catalyst deactivation, the following relation is obtained:

$$\frac{\partial C_i}{\partial t} = -u\frac{\partial C_i}{\partial z} - C_i\frac{\partial u}{\partial z} - \frac{1-\varepsilon}{\varepsilon}\rho\left[-r(C_i,T)\right]a \qquad (5)$$

Boundary conditions:

$$at \;\; t=0 \;\; , \;\; z=0 \qquad \Rightarrow C_i = C_{i,in}$$
$$at \;\; t=t \;\; , \;\; z=L \qquad \Rightarrow C_i = C_{i,out}$$

Under the experimental conditions applied in this study, the catalysts activity remained unchanged during a period of 12 hours (Fig.2, Temperature=250 °C). The catalyst deactivation was, therefore, ignored (a =1). In addition, the mean diameter of catalyst particles was 100 μm and was loaded in the reactor as fine powders. The overall effectiveness factor (η) was assumed equal to unity. In other words, it may be assumed that neither internal nor external diffusion have been effective within the process.

By considering a dimensionless coordinate ξ=z/L; β= (1-ε)/ε, Isothermal condition and the ideal gas law, equation (5) may be rearranged as follows:

$$\frac{\partial P_i}{\partial t} = -\frac{u}{L}\frac{\partial P_i}{\partial \xi} - \frac{P_i}{L}\frac{\partial u}{\partial \xi} - \beta.\rho.RT(-r_i) \qquad (6)$$

Furthermore, in the case of chemical reactions with density change, the term $(\partial u/\partial \xi)$ can be expressed as a function of $(\partial P_i/\partial \xi)$, applying the following two relations:

$$u = u_0(1+\varepsilon_{CO}.X_{CO}) \qquad (7)$$

$$P_{CO} = P_{CO}^0\frac{1-X_{CO}}{1+\varepsilon_{CO}X_{CO}} \qquad (8)$$

and

$$P_{DME} = P_{CO}^0\frac{X_{CO}.X_M}{2(1+\varepsilon_{CO}.X_{CO})} \qquad (9)$$

Substitution of equations (7) and (8) in (6), after some simple mathematical manipulations, yields the following relation:

$$\frac{\partial X_{CO}}{\partial t} = -\frac{u_0(1+\varepsilon_{CO}X_{CO})^2}{L(1+\varepsilon_{CO})}\frac{\partial X_{CO}}{\partial \xi} + \frac{(1+\varepsilon_{CO}X_{CO})^2}{P_{CO}^0(1+\varepsilon_{CO})}\beta.\rho.RT(-r_{CO}) \tag{10}$$

Similarly, mathematical manipulation and substitution of equations (7) and (9) in (6) results in equation (11):

$$\frac{P_{CO}^0.X_{CO}}{(1+\varepsilon_{CO}.X_{CO})}\frac{\partial X_M}{\partial t} + \frac{P_{CO}^0 X_M}{(1+\varepsilon_{CO}X_{CO})^2}\frac{\partial X_{CO}}{\partial t} = -\frac{u_0 P_{CO}^0}{L}\left(X_{CO}\frac{\partial X_M}{\partial \xi} + X_M\frac{\partial X_{CO}}{\partial \xi}\right) - 2\beta.\rho.RT(r_{DME}) \tag{11}$$

Finally, applying equation (10) in equations (11) gives the following result:

$$\frac{\partial X_M}{\partial t} = -\frac{u_0(1+\varepsilon_{CO}X_{CO})}{L}\frac{\partial X_M}{\partial \xi} - \frac{u_0\varepsilon_{CO}X_M(1+\varepsilon_{CO}X_{CO})}{L.X_{CO}(1+\varepsilon_{CO})}\frac{\partial X_{CO}}{\partial \xi} - \frac{(1+\varepsilon_{CO}X_{CO})\beta.\rho.RT}{P_{CO}^0.X_{CO}}\left[\frac{X_M}{1+\varepsilon_{CO}} + 2\right](r_{DME}) \tag{12}$$

By replacing ($-r_{CO}$) from equation (3) and (r_{DME}) from equation (4) in equations (10) and (12) respectively, the following relations may be obtained:

$$\frac{\partial X_{CO}}{\partial t} = f_1(X_{CO}) * \left[\frac{X_{CO}(m+1) - X_{CO}(m)}{\Delta \xi}\right] + f_2(X_{CO}, X_M) \tag{13}$$

$$\frac{\partial X_M}{\partial t} = f_3(X_{CO})\left[\frac{X_M(m+1) - X_M(m)}{\Delta \xi}\right] - f_4(X_{CO}, X_M) * \left[\frac{X_M(m+1) - X_{CO}(m)}{\Delta \xi}\right] + f_5(X_{CO}, X_M) \tag{14}$$

These two equations have been solved simultaneously using Matlab software (Version 7.02). The results are presented in Figures 3-12.

4-3. Applications of model

4-3-1. Variation of CO conversion at the reactor outlet

In Figure 3, the experimental data for CO conversion at the reactor outlet and those predicted from the model are presented. Apart from the initial period, the correlation between the two sets of data is satisfactory in all experimental runs. The discrepancies observed in the initial period may be either due to the use of steady state experimental results in the prediction of system behavior under unsteady state conditions, or to the experimental errors involved in the determination of transient CO concentrations at the reactor outlet.

4-3-2. Variation of methanol and DME partial pressures at the reactor outlet

The experimental data for partial pressures of methanol and DME at the reactor outlet and those estimated from the model are given in Figs 4 and 5. Similar to the previous case, apart from the initial period, the correlations between the experimental and predicted values are fairly good. The discrepancies observed at the earlier stages could be related to the application of steady state experimental data in the prediction of system behavior under unsteady state conditions.

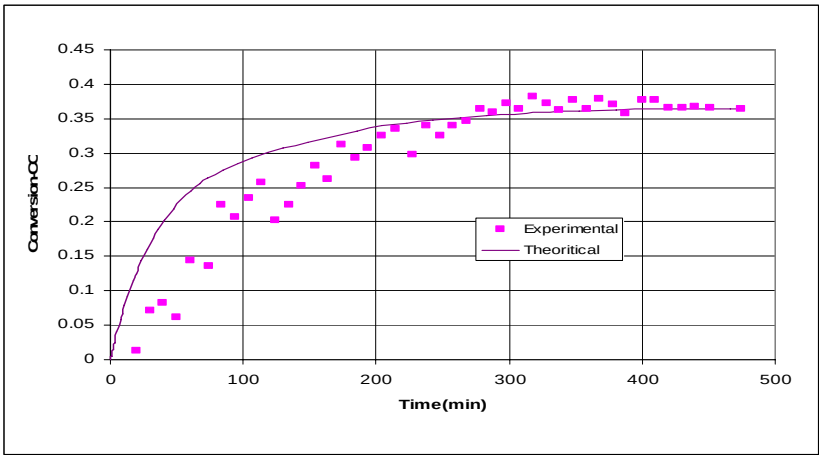

Figure 3. Conversion of CO as a function of time at the reactor outlet (T=250 °C, W/F=1120 g/(mol/min)).

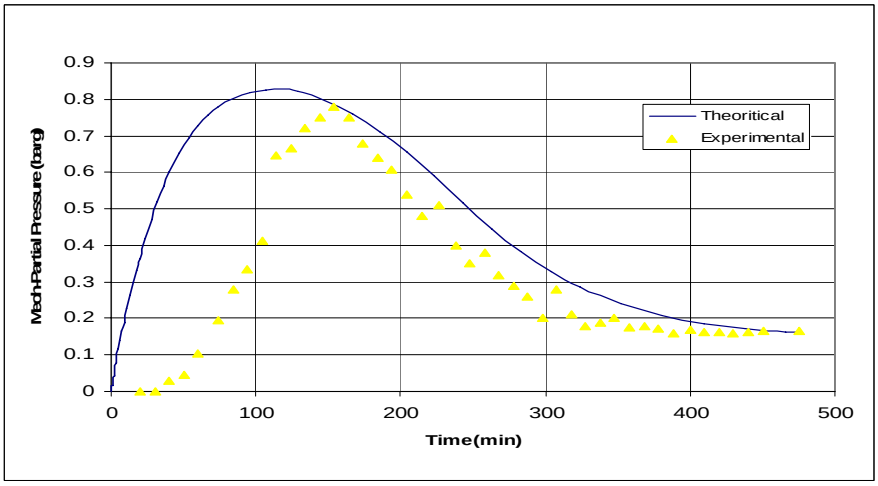

Figure 4. Partial pressure of methanol as a function of time at the reactor outlet (T=250 °C, W/F=1120 g/(mol/min)).

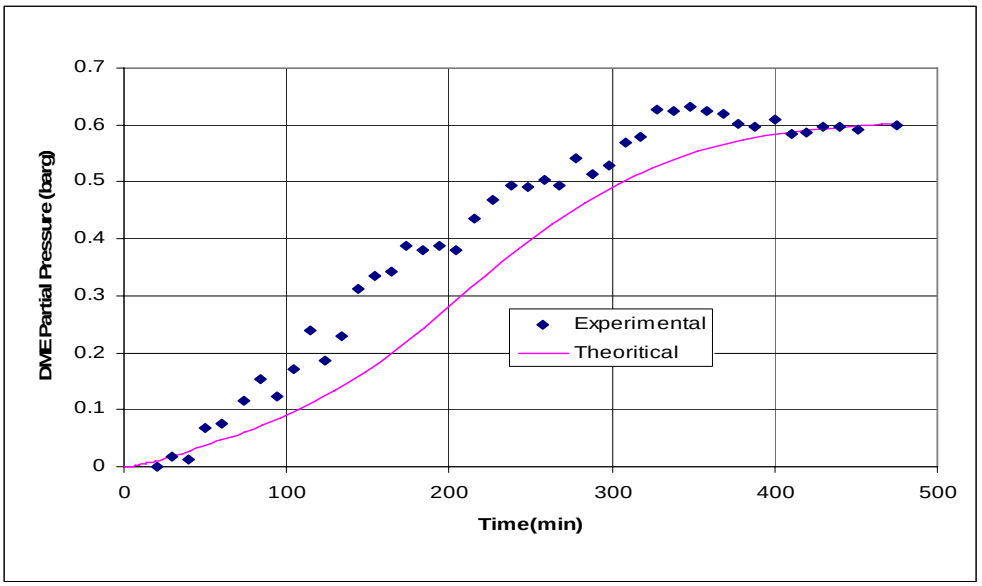

Figure 5. Partial pressure of DME as a function of time at the reactor outlet (T=250 °C, W/F=1120 g/(mol/min)).

4-3-3. Variation of CO conversion within the reactor

Conversions of CO at different depths of the catalyst bed, as calculated from the model, are plotted in Fig.6. Each curve in Fig.6 represents a specific location within the reactor. The conversions at each location have been calculated at different times after the start of the experiment.

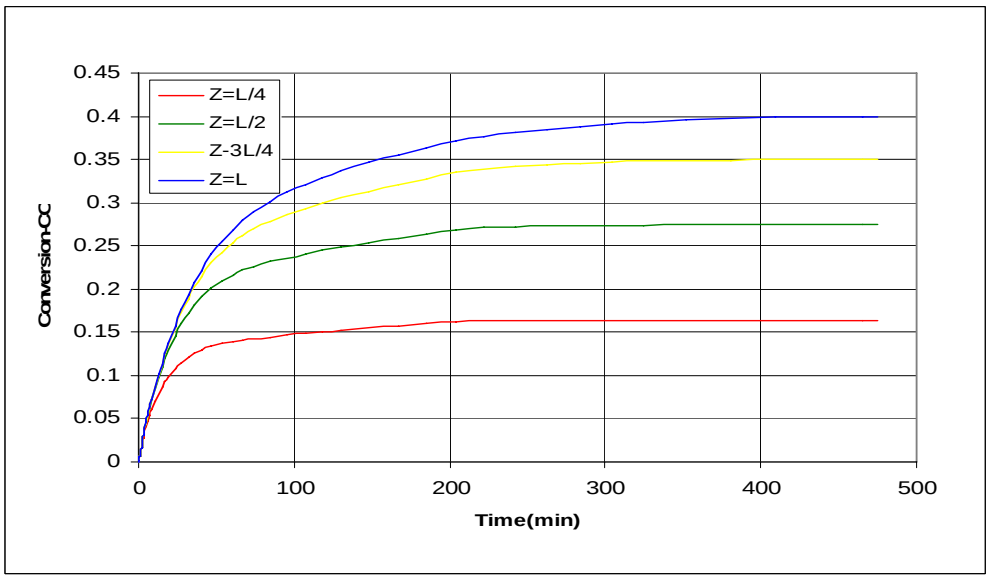

Figure 6. Conversion of CO as a function of time at different depths of catalyst bed (T=250 °C, W/F=1120 g/(mol/min)).

4-3-4. Variation of methanol and DME partial pressures within the reactor

Predicted data for the methanol and DME partial pressures at different depths of the catalyst bed against time are plotted in Figures 7 and 8, respectively.

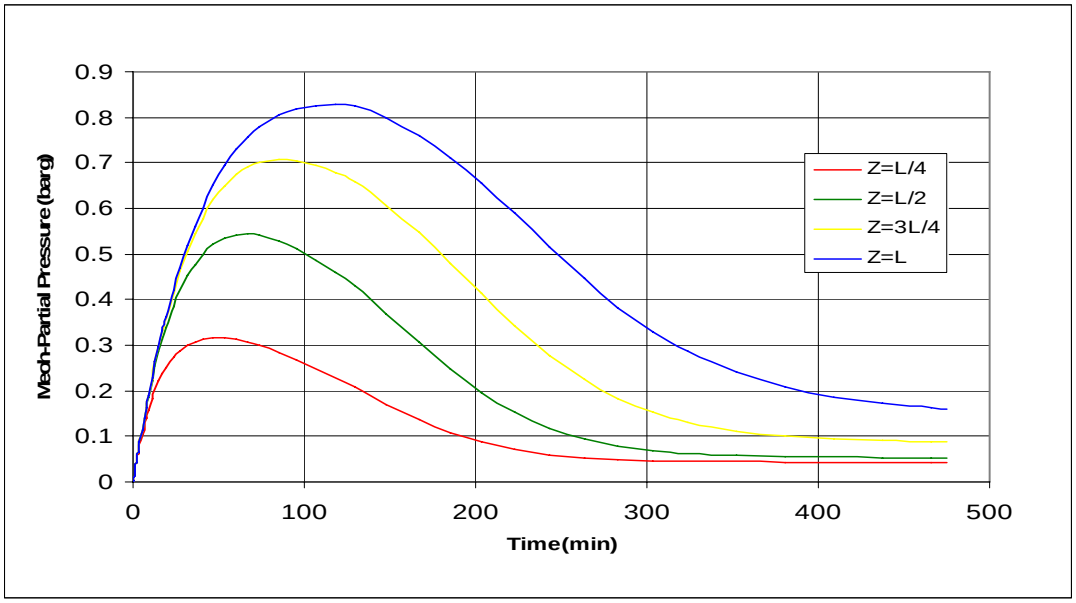

Figure 7. Partial pressure of methanol as a function of time at different depths of catalyst bed (T=250 °C, W/F=1120 g/(mol/min)).

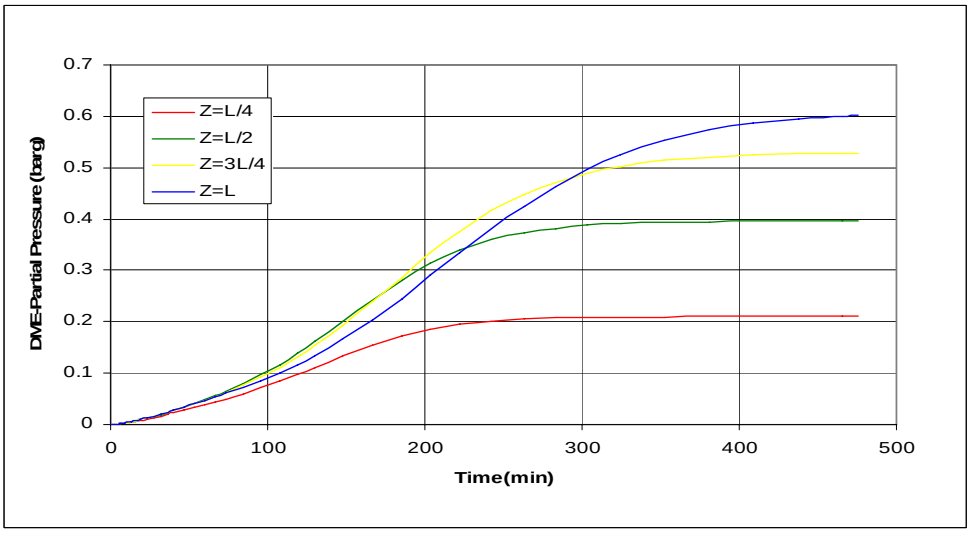

Figure 8. Partial pressure of DME as a function of time at different depths of catalyst bed (T=250 °C, W/F=1120 g/(mol/min)).

4-3-5. Variation of CO conversion along the reactor

Conversions of CO as a function of both time and reactor length are given in Fig.9.

4-3-6. Variation of methanol and DME partial pressures along the reactor

At a certain time after the start of each experiment, the partial pressures of DME and methanol at different locations within the reactor have been calculated using the dynamic model. Predicted data for partial pressures of methanol, as a function of time and reactor length, before and after extermum point, are presented in Figs 10 and 11, respectively. Whereas the data for DME is plotted in Fig. 12.

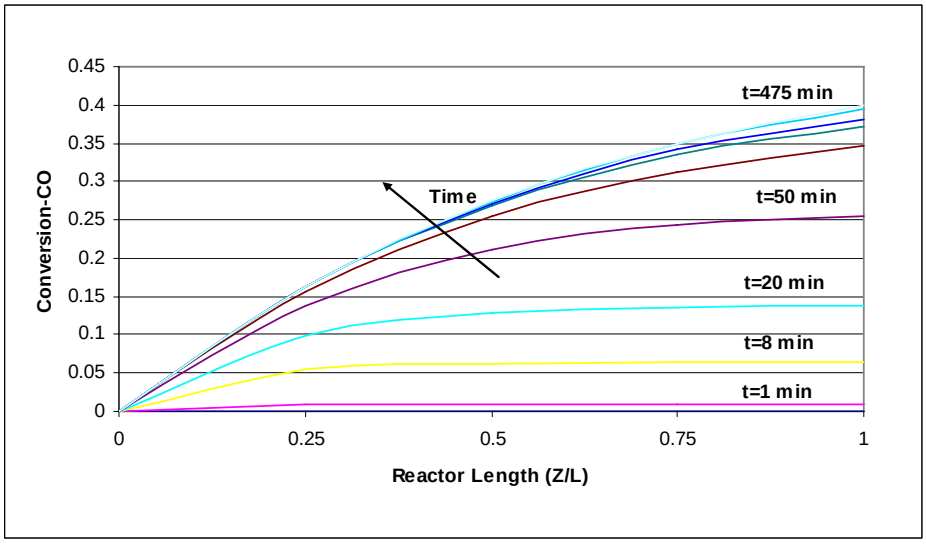

Figure 9. Conversion of CO along the reactor (T=250 °C, W/F=1120 g/(mol/min)).

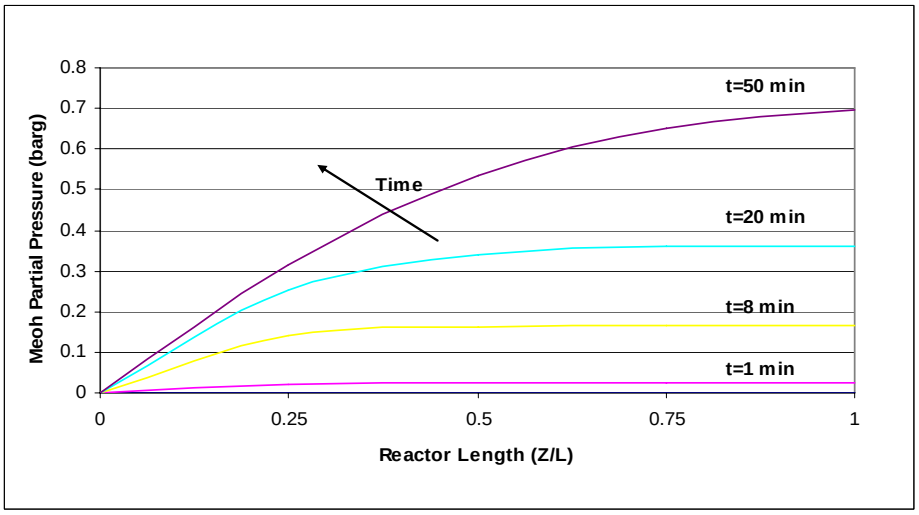

Figure 10. Partial pressures of methanol along the reactor (before extermum point-T=250 °C, W/F=1120 g/(mol/min)).

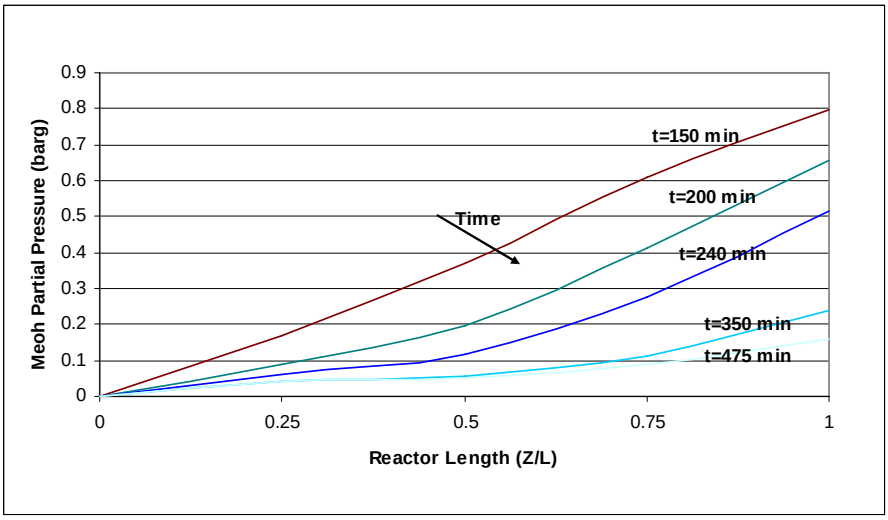

Figure 11. Partial pressures of methanol along the reactor (after extermum point-T=250 °C, W/F=1120 g/(mol/min)).

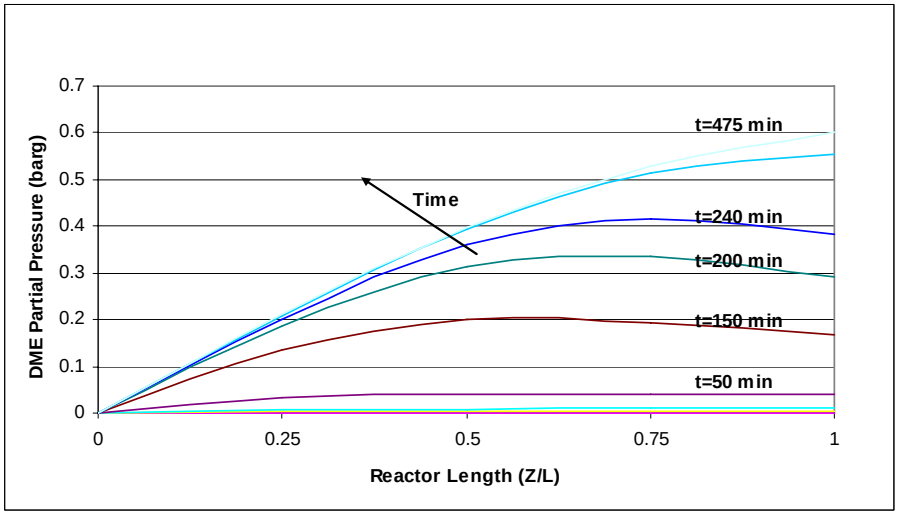

Figure 12. Partial pressures of DME along the reactor (T=250 °C, W/F=1120 g/(mol/min)).

5. Conclusion

A kinetic expression for syngas trans-formation to DME based upon Graff methanol synthesis and Bercic dehydration models has been derived and correlated with the experimental results over a range of temperatures. In order to predict the behavior for the process of direct conversion of synthesis gas to DME in a packed bed catalytic reactor, a simple dynamic model has been put forward. The data predicted from the model were correlated with those determined experimentally. The degree of agreement between the two sets of data, for the steady state conditions, was 85-95% and the mean absolute error for dynamic conditions was 14%. This model may be thus applied to predict the optimum operating temperature and depth of a catalyst bed required for such a process.

6. Symbols

a	Catalyst activity
C	Concentration (mol/cm$^{3)}$
F	Molar flow rate (mol/min)
f	Denotes function
k	Kinetic parameters
K_p	Equilibrium constant
L	Reactor length (mm)
m	Exponent in equations (14) and (15)
P	Pressure (barg)
r	Reaction rate (mol/min.$g_{cat.}$)
R	Universal gas constant (J/mol.K)
t	Time (min)
T	Temperature (K)
u	Surface velocity of gases (mm/min)
W	Catalyst mass (g)
X	Conversion
y	Mole fraction
z	Longitudinal coordinate along the reactor (mm)

Subscript

i	ith component
M	Methanol

Greek letters

β	Constant
ε	Bed porosity
ε_{co}	Expansion parameter
ϕ_v	Volumetric flow rate (m^3/min)
ρ	Bulk density (g/cm^3)
ξ	Dimensionless coordinate along the reactor
η	Effectiveness factor

7. References

1. Hansen, J., Voss, B., Joensen, F. and Dcra-Siguroavdottir, I. "Large Scale Manu Facture of DME a New alternative Diesel Fuel From Natural gas", *International Congress & Exposition, Detroit – Michigan*, Feb. 27-March2 (1995).
2. Smadani, S. G. "Chementator", *Chem. Eng. April*, (1995), 17-18.
3. Fleisch, T., McCarthy, C., Basu, A. and Udovich, C. "Demonstration of
4. ULEV Emissions on a Navistar Diesel Engine Fueled with Dimethyl Ether", SAE Technical Paper Series, *International Congress & Exposition, Detroit, Michigan*, February 27-March 2,1995.
5. Nle, Z., Liu, H., Liu, D., Ying, W. and Fang, D. "Intrinsic Kinetics of Dimethyl Ether Synthesis From Syngas", *J. of Natural gas Chemistry*, 14(2005), 22-28.
6. Ge, Q., Huang, Y., Qiu, F. and Li, S. "Bifunctional catalysts for conversion of synthesis gas to DME", *Applied Catalysis*, 167, 1998, 23-30.
7. Hadipour, A. and Sohrabi, M. " Synthesis of Some Bifunctional Catalysts for Direct Conversion of Syngas to DME as a Clean Diesel Fuel", Paper Accepted for Presentation at the *First International Congress on Green Process Engineering* to be Held in Toulous-France, 24-26 April, 2007.
8. Bercic, G. and Levec, J. "Intrinsic and Global reaction rate of Methanol Dehydration Over γ-Al_2O_3 Pellets", *Ind. Eng. Chem. Res*. 31 (1992), 1035-1040.
9. Bercic, G. and Levec, J. "Catalytic Dehydration of Methanol to DME. Kinetic Investigation and Reactor Simulation", *Ind. Eng Chem. Res.* 32 (1993), 2478-2484.
10. Erena, J., Arandes, J. M., Bilbao, J., Gayubo, A. G. and De lasa, H. I. "Conversion of Syngas to Liquid Hhydrocarbons Over a Two-Component (Cr_2O_3-zno and zsm-5 zeolite) Catalyst: Kinetic Modeling and Catalyst Deactivation", *Chem. Eng. Sci*., 55 (2000), 1845-1855.
11. Peng, X. D., Toseland, B. A. and Tijm, P. J. A. "Kinetic Understanding of Chemical Synergy under LPDME Conditions – Once Through Applications", *Chem. Eng. Sci*., 54 (1999), 2787-2792.
12. Graaf, G. H., Winkelman, J. G.M., Stamhuis, E. J. and Beenakers, A. A. C. M. "Kinetics of Three Phase Methanol Synthesis", *Chem. Eng. Sci*., 43, 8 (1988), 2161-2168.
13. Graaf, G. H., Sijtsema, P. J. J. M., Stamhuis, E. J. and Joosten, G. E. H. "Chemical Equilibria In Methanol Synthesis", *Chem. Eng. Sci*., 41, 11 (1986), 2883-2890.
14. Graaf G. H., Stamhuis, E. J. and Beenakers, A. A. C. M. "Kinetics of Low-Pressure Methanol Synthesis", *Chem. Eng. Sci.,* 43, 12 (1988), 3185-3195.